

## A TOPOLOGICAL ASYMPTOTIC ANALYSIS FOR THE REGULARIZED GREY-LEVEL IMAGE CLASSIFICATION PROBLEM\*

DIDIER AUROUX<sup>1</sup>, LAMIA JAAFAR BELAID<sup>2</sup> AND MOHAMED MASMOUDI<sup>1</sup>

**Abstract.** The aim of this article is to propose a new method for the grey-level image classification problem. We first present the classical variational approach without and with a regularization term in order to smooth the contours of the classified image. Then we present the general topological asymptotic analysis, and we finally introduce its application to the grey-level image classification problem.

**Mathematics Subject Classification.** 35Q80, 49J20, 49K20, 65-04, 68-04, 68U10.

Received October 28, 2005. Revised January 15, 2007.

### 1. INTRODUCTION

The goal of topological optimization and most image processing problems is to create a partition of a given domain (or set):

- In topological optimization, for a given domain  $\Omega$ , we look for the optimal design  $\omega \subset \Omega$  and its complementary;
- In image processing problems like edge detection, classification, and segmentation, the goal is to split the image in several parts.

For this reason, topological shape optimization and image processing problems have common mathematical methods like level set approaches, material properties optimization, variational methods, ...

Level set approaches have been applied to image processing [8, 9, 24, 28, 30] and it gave very promising results in topological shape optimization [3, 4, 34]. Diffusive methods in image restoration are based on the optimization of conductive material properties [8, 35]. Like in topological optimization [1, 10], isotropic and anisotropic [26] approaches are considered.

In this paper, we consider the topological gradient approach that has been introduced for topological optimization purpose [2, 6, 19, 22, 27, 31]. It has been applied to diffusive image restoration giving very promising results [20]. An optimal material distribution is obtained at the first iteration. Our objective is to apply topological gradient approach to image classification.

This paper is concerned with the problem of classifying an image according to  $n$  predefined grey level intensities  $C_i$ ,  $1 \leq i \leq n$ . Let us first recall the general mathematical formulation of image classification

---

*Keywords and phrases.* Image classification, topological asymptotic expansion, image restoration.

\* *The authors would like to thank the referees for their helpful comments and suggestions.*

<sup>1</sup> Institut de Mathématiques de Toulouse, UMR 5219, Université Paul Sabatier Toulouse 3, 31062 Toulouse cedex 9, France. [auroux@mip.ups-tlse.fr](mailto:auroux@mip.ups-tlse.fr); [masmoudi@mip.ups-tlse.fr](mailto:masmoudi@mip.ups-tlse.fr)

<sup>2</sup> ENIT-LAMSIN, BP37, 1002 Tunis Belvédère, Tunisia. [lamia.belaid@esstt.rnu.tn](mailto:lamia.belaid@esstt.rnu.tn)

© EDP Sciences, SMAI 2007

problem. Let  $\Omega$  be an open bounded domain of  $\mathbb{R}^2$  and let  $u_0 : \Omega \rightarrow \mathbb{R}$  be the observed data function (the grey level intensity). The classification problem consists in finding a regular and homogeneous partition of  $\Omega$ . A partitioning of  $\Omega$  consists in searching for a family of open sets  $\{\omega_i\}_{i=1,\dots,n}$ , such that  $\omega_i \cap \omega_j = \emptyset$  if  $i \neq j$ , and  $\Omega = \cup_{i=1}^n \omega_i \cup \Gamma$ . The set  $\Gamma$  is the union of all interfaces between two different subsets:  $\Gamma = \cup_{i \neq j} \Gamma_{ij}$  where  $\Gamma_{ij}$  represents the interface between  $\omega_i$  and  $\omega_j$ . A regular partition means that  $\Gamma$  is of minimal length and an homogeneous partition means that in each set  $\omega_i$  the grey level intensity is close to  $C_i$  in the  $L^2$  norm sense.

Many classification models have been studied and tested on synthetic and real images in image processing literature, and results are more or less comparable considering the complexity of the suggested algorithms and/or the implementation cost. We can cite here some models widely used like the structural approach by regions growth [25], the stochastic approaches [11, 12, 16, 17, 21] and the variational approaches which are based on various strategies like level set formulations, the Mumford-Shah functional, active contours and geodesic active contours methods or wavelet transforms [7–9, 23, 24, 28, 29, 35].

The goal of this paper is to solve a grey-level image classification problem using the topological gradient method [4, 5, 10, 18, 19, 22]. The basic idea of this method is to minimize a cost function  $j(\Omega) = J(u_\Omega)$  where  $u_\Omega$  is the solution of a partial differential equation defined in the domain  $\Omega$ . In order to minimize  $j$ , one starts by creating a hole  $x_0 + \rho\mathcal{B}$  around a point  $x_0$  in the domain  $\Omega$ , where  $\mathcal{B}$  is a non-empty open set which contains the origin  $O$ , and measuring the impact of such a modification of the domain on the cost function. This provides an asymptotic expansion of  $j(\Omega \setminus \overline{x_0 + \rho\mathcal{B}}) - j(\Omega)$  when  $\rho \rightarrow 0$ . In most cases, it is possible to obtain an asymptotic behavior of the form  $j(\Omega \setminus \overline{x_0 + \rho\mathcal{B}}) - j(\Omega) = f(\rho).g(x_0) + o(f(\rho))$ , where  $f$  is a positive function which satisfies  $f(\rho) \rightarrow 0$  when  $\rho \rightarrow 0$ , and  $g$  is then called the topological gradient. Since  $f$  is positive, the idea is to find the set of points  $x$  where the topological gradient is negative, and then to create holes around these points in order to minimize  $j$ .

In the present work, we are interested in using such a method for the classification of grey-level images. We will initially assume that the classification is supervised, *i.e.* the number and values of the classes are given, and we first propose a method based on the topological gradient theory to regularize the classification process, in order to obtain smoother contours. Then we propose a classification model based on a restoration process, still using the topological asymptotic expansion. Finally we propose an improvement which gives much smoother contours. In the concluding remarks, we briefly propose a method for finding the *optimal* number and values of the classes if they are not given (unsupervised classification).

## 2. VARIATIONAL CLASSIFICATION FORMULATION

### 2.1. Without regularization

Let  $u_0$  be the original image defined on an open set  $\Omega$  of  $\mathbb{R}^2$ . We want to classify the image  $u_0$  using  $n$  predefined classes  $C_i$ ,  $1 \leq i \leq n$ , and we choose the grey level intensity as a classifier. The goal of image classification is then to find a partition of  $\Omega$  in subsets  $\{\omega_i\}_{i=1,\dots,n}$ , such that  $u_0$  is close to  $C_i$  in  $\omega_i$ . The classified image  $u$  will then be defined by

$$u(x) = C_i \quad \forall x \in \omega_i, \quad (1)$$

where  $\{\omega_i\}_{i=1,\dots,n}$  are defined by

$$\omega_i = \{x \in \Omega; x \text{ belongs to the } i\text{th class}\}. \quad (2)$$

The variational approach consists in minimizing a cost function measuring the mean square difference between the original image and the classified image

$$j(\omega) = \sum_{i=1}^n \int_{\omega_i} (u_0(x) - C_i)^2 dx, \quad (3)$$

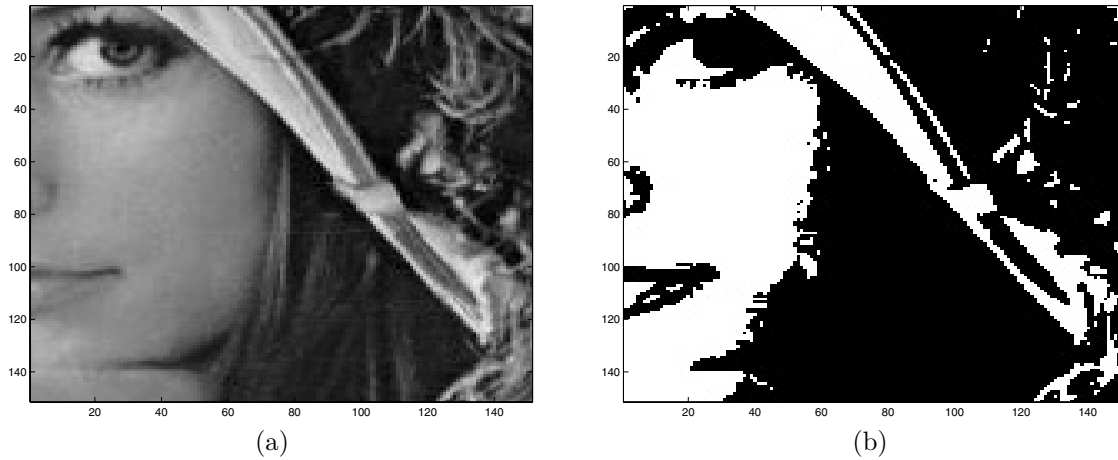


FIGURE 1. Original image (a) and 2-classes ( $C = \{0; 255\}$ ) classified image obtained using the *closest class* algorithm (b).

where  $\omega = (\omega_1, \dots, \omega_n)$  is a partition of  $\Omega$ .

The minimization of  $j$  is easy, because it is a separable cost function; for each point  $x \in \Omega$ , we only have to find  $i_x = \arg \min\{|u_0(x) - C_i|; i = 1, \dots, n\}$  and add  $x$  to subset  $\omega_{i_x}$ . This can be called the *closest class* algorithm because each pixel of the original image is assigned in the classified image to its closest class.

Figure 1a shows the original  $151 \times 151$  image  $u_0$ , using 256 grey levels: the grey level of a pixel is an integer  $u_0(x) \in \{0; 255\}$ . We have chosen  $C_1 = 0$  (black) and  $C_2 = 255$  (white). Figure 1b shows the computed image using the *closest class* algorithm.

## 2.2. With regularization

In order to obtain a classified image with smoother contours, we may add a regularization term to the cost function

$$j(\omega) = \sum_{i=1}^n \int_{\omega_i} (u_0(x) - C_i)^2 dx + \alpha \sum_{i \neq j} |\Gamma_{ij}|, \quad (4)$$

where  $|\Gamma_{ij}|, i \neq j$  represents the one-dimensional Hausdorff measure of  $\Gamma_{ij}$  [8], and  $\alpha$  is a positive regularization parameter. It can be understood as a weighting factor between the initial objective function (Eq. (3), without regularization) and the regularization term.

This equation corresponds to the Mumford-Shah energy with a piecewise constant function [14, 23, 32, 33]. In order to solve this problem, variational models were proposed [28, 29]. The minimization of  $j$  is no more easy to compute, the main difficulty comes from the fact that the unknowns are sets and not variables. It is then possible to use the topological gradient theory to solve the regularized classification problem.

## 3. TOPOLOGICAL GRADIENT FOR THE IMAGE CLASSIFICATION

The classification model that we propose is based on the topological gradient method [27]. In fact, to assign each pixel of the original image to one of the classes  $C_i, 1 \leq i \leq n$ , it suffices to suppose first that all pixels are assigned to the same class, and then to find subsets of pixels that should be reassigned to the other classes.

### 3.1. Mathematical formulation of the problem

Let  $\Omega$  be a bounded domain of  $\mathbb{R}^2$  and  $\partial\Omega$  its boundary. It is the domain definition of the image  $u_0$ , which can be understood as a function  $u_0 : x \in \Omega \mapsto u_0(x)$ , where  $u_0(x)$  is the grey level of the image  $u_0$  at the point  $x$ .

From the numerical point of view, the image is defined by a finite element formulation. The domain  $\Omega$  is a square and it is decomposed in a grid of identical elementary squares. The image  $u_0$  is then a polynomial of type  $Q1$  in each element. In the following we refer to each element or pixel by its centre  $x$  and the set  $\mathcal{B}$  will be the classical reference element [13, 15].

We also assume that we have given classes  $(C_1, \dots, C_n)$ .

We are looking for a partition of the domain  $\Omega$  into subsets  $(\omega_i)_{i=1, \dots, n}$  so that if we denote by  $u$  the following piecewise constant function:

$$u = \begin{cases} C_1 & \text{in } \omega_1, \\ \vdots & \\ C_{n-1} & \text{in } \omega_{n-1}, \\ C_n & \text{in } \omega_n = \Omega \setminus \left( \bigcup_{i=1}^{n-1} \overline{\omega_i} \right), \end{cases} \quad (5)$$

then  $u$  is close to the original image  $u_0$ .  $u$  will be further called the classified image. In the previous equation,  $\omega_i$  represents the subset of pixels that should be reassigned to the class  $C_i$ . The unknowns are then the open subsets  $\omega_i$  constituting the partition of  $\Omega$ .

We first work with the cost function without a regularization term, measuring the mean square difference between the solution  $u$  (classified image) of (5) and the original image  $u_0$

$$J(u) = \int_{\Omega} |u - u_0|^2 dx. \quad (6)$$

As the solution  $u$  of equation (5) depends only on the choice of the partition  $\omega = (\omega_1, \dots, \omega_n)$ , the cost function  $J$  can be understood as a function depending only on the partition  $\omega$

$$j(\omega) := J(u) = \int_{\Omega} |u - u_0|^2 dx. \quad (7)$$

Finding a classified image  $u$ , close to the original function (the original image  $u_0$ ) is then equivalent to minimizing the cost function  $j$ , with respect to the partition  $\omega$ .

In the case of a regularized classification problem, we will add a regularization term in the cost function:

$$j(\omega) = \int_{\Omega} |u - u_0|^2 dx + \alpha \sum_{i \neq j} |\Gamma_{ij}|, \quad (8)$$

where the coefficient  $\alpha$  and the interfaces  $\Gamma_{ij}$  are defined as in the previous section.

The initialization is performed with the following partition:  $\omega = (\emptyset, \dots, \emptyset, \Omega)$ , *i.e.* all pixels are assigned to the last class  $C_n$ .

### 3.2. Variation of the cost function

#### 3.2.1. Without regularization

In the present case, the topological expansion analysis gives no real improvement compared to a classical minimization approach because it is possible to calculate exactly the variation of the cost function. It is indeed

possible to study the variations of  $j$  (defined in Eq. (7)) when we switch, in a small region,  $u$  from class  $n$  to class  $i, i \neq n$ . The small region is given by  $\mathcal{B}_{x,\rho} = x + \rho\mathcal{B}$  and the variation of  $j$  is

$$\delta j_i(x, \rho) := j(\omega_1, \dots, \omega_i \cup \mathcal{B}_{x,\rho}, \dots, \omega_n \setminus \overline{\mathcal{B}_{x,\rho}}) - j(\omega_1, \dots, \omega_n) = \int_{\Omega} |u_{new} - u_0|^2 dx - \int_{\Omega} |u_{old} - u_0|^2 dx, \quad (9)$$

where  $u_{new}$  and  $u_{old}$  are the solutions of equation (5) with these two partitions respectively. Hence,  $u_{new} = u_{old}$  except on  $\mathcal{B}_{x,\rho}$  where  $u_{new} = C_i$  and  $u_{old} = C_n$ . Then, the variation of the cost function is

$$\delta j_i(x, \rho) = \int_{\mathcal{B}_{x,\rho}} (C_i - u_0)^2 - (C_n - u_0)^2 dx = \rho^2 |\mathcal{B}| ((C_n - C_i)^2 - 2(C_n - C_i)(C_n - u_0(x))) + o(\rho^2), \quad (10)$$

if  $u_0$  is regular (Lipschitz).

From the discrete point of view (*i.e.* considering the image formulation),  $\mathcal{B}_{x,\rho}$  represents the pixel  $x$  and the topological gradient is then given by

$$g_i(x) = (C_n - C_i)^2 - 2(C_n - C_i)(C_n - u_0(x)), \quad (11)$$

and  $f(\rho) = \rho^2 |\mathcal{B}|$ .

The implementation of this method is quite easy, because we only have to compute each  $g_i$ , which is an affine function of the original image  $u_0$ , and then find the pixels  $x$  where  $g_i(x) < 0$ , in order to minimize the cost function  $j$ , and reassign them to the optimal class.

The algorithm is then the following.

### Algorithm

- For  $1 \leq i \leq n - 1$ , compute  $g_i(x)$  for each pixel  $x$ ;
- for each pixel  $x$ , find  $i_0$  so that  $g_{i_0}(x) \leq g_i(x) \forall i$ ;
- if  $g_{i_0}(x) < 0$ , reassign  $x$  to the class  $C_{i_0}$ .

It is easy to see that this algorithm converges in one iteration, and that at the end of the process, each pixel is reassigned to its closest class, *i.e.* to the class  $C_{i_0}$  with  $i_0 = \arg \min\{|C_i - u_0(x)|^2\}$ . Hence the algorithm converges towards a global minimum of the cost function (3).

### 3.2.2. With regularization

If we add a regularization term to the cost function, we can still use the previous algorithm, but it will no more converge in only one iteration. For a given  $x$  in  $\omega_j$  ( $j$  not necessary equal to  $n$ ), the variation of the cost function upon reassigning the pixel  $x$  to class  $i$  is now given by

$$\delta j_i(x) = \rho^2 |\mathcal{B}| (C_j - C_i)(2u_0(x) - C_i - C_j) + \alpha \rho |\partial \mathcal{B}| (1 - \delta_{ij}) + o(\rho^2), \quad (12)$$

where  $\delta_{ij}$  stands for the Kronecker symbol; if  $i = j$  the perimeter remains unchanged. When  $x$  is located at the interface between at least two classes, we derive a similar expansion.

At first sight, this second order expansion seems to be inappropriate for numerical applications. In our knowledge, only the leading term of topological expansions has been considered up to now. We propose to consider  $\rho_0$  and  $\mathcal{B}$  such that  $\mathcal{B}_{x,\rho_0}$  has exactly the shape of pixel a  $x$ . We propose the following generalization of the topological gradient

$$g_i(x) = \rho_0^2 |\mathcal{B}| (C_j - C_i)(2u_0(x) - C_i - C_j) + \alpha \rho_0 |\partial \mathcal{B}| (1 - \delta_{ij}). \quad (13)$$

The classical topological gradient is the particular case when only the leading term of the expansion is considered and  $\rho_0$  is fixed such that  $f(\rho_0) = 1$ .

The pixel  $x$  is still reassigned to the class  $i_0$  that minimizes the topological gradient  $g_i(x)$  with respect to  $i$ .

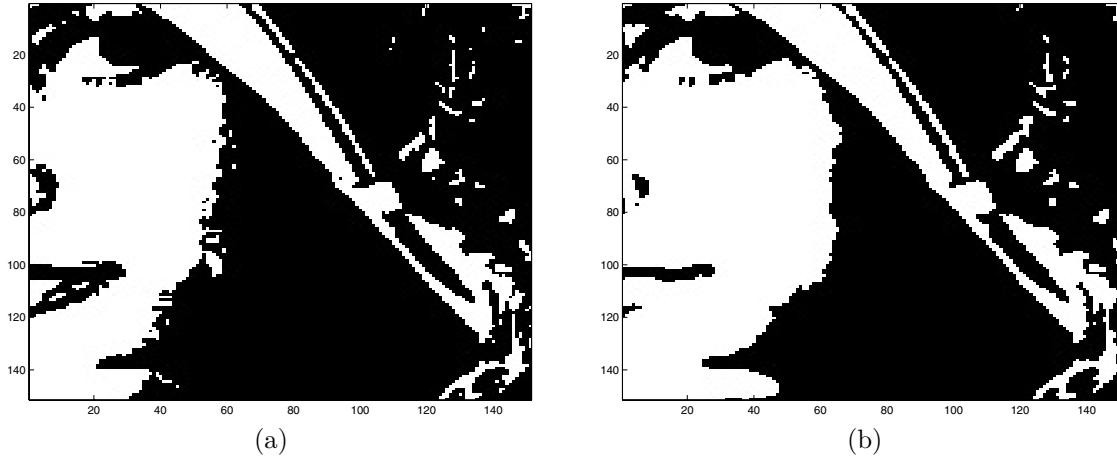


FIGURE 2. Two-classes classified images obtained using the topological gradient algorithm: unregularized (a) and regularized (b).

Because of the regularization term, it is interesting to use the unregularized classified image as an initial guess, and the minimization process will need more than one iteration because some pixels which had positive topological gradients may have negative ones at next iteration. If for example all neighbors of  $x$  have been reassigned to class  $i$  but not  $x$ , which is still assigned to the class  $C_n$ , at the next iteration, the regularization term in  $\delta j_i(x)$  may be strongly negative, and then  $x$  may be reassigned to the class  $C_i$ . So, we have to iterate the algorithm until all functional variations  $\delta j_i$  are everywhere non negative.

The numerical convergence of this algorithm is ensured by the fact that the set of possible partitions  $\omega$  is finite. It is equal to  $n^N$ , where  $N$  is the number of image pixels. Then the algorithm stops or goes into a cyclic loop. If the cost function decreases strictly at each iteration, the algorithm stops after a finite number of iterations.

However the convergence towards the global minimum of the regularized cost function is no more ensured, but this algorithm is nevertheless quite commonly used [28], and as we use the unregularized classified image as an initial guess for the minimization algorithm, we obtain quite good numerical results (see next paragraph).

### 3.3. Numerical results

Figure 2a shows the computed image using the topological gradient algorithm with the unregularized cost function and  $n = 2$  classes ( $C = \{0; 255\}$ ). This obviously gives the same result as the closest class algorithm because the asymptotic expansion of the unregularized cost function is indeed an exact variation. Figure 2b shows the result of the topological gradient algorithm with the regularized cost function. We can clearly see that the resulting image has smoother contours and fewer isolated points. The minimization of the regularized cost function was achieved in less than ten iterations.

Figure 3 shows the same results as in Figure 2 for 3 and 5 classes. The conclusions are obviously the same.

Although this method is based on the asymptotic expansion theory, it has two main disadvantages: we are not sure to obtain the global minimum of the cost function, and the convergence is not achieved in one iteration. We will now apply the topological gradient theory in another context.

## 4. A REGULARIZED CLASSIFICATION MODEL BASED ON A RESTORATION PROCESS

Inspired by the work of G. Aubert *et al.* [8, 29] in which the authors propose a classification model coupled with a restoration process, we propose in this section to use the topological gradient approach applied to image restoration problem [20] for the regularized classification problem. We begin first by recalling the application

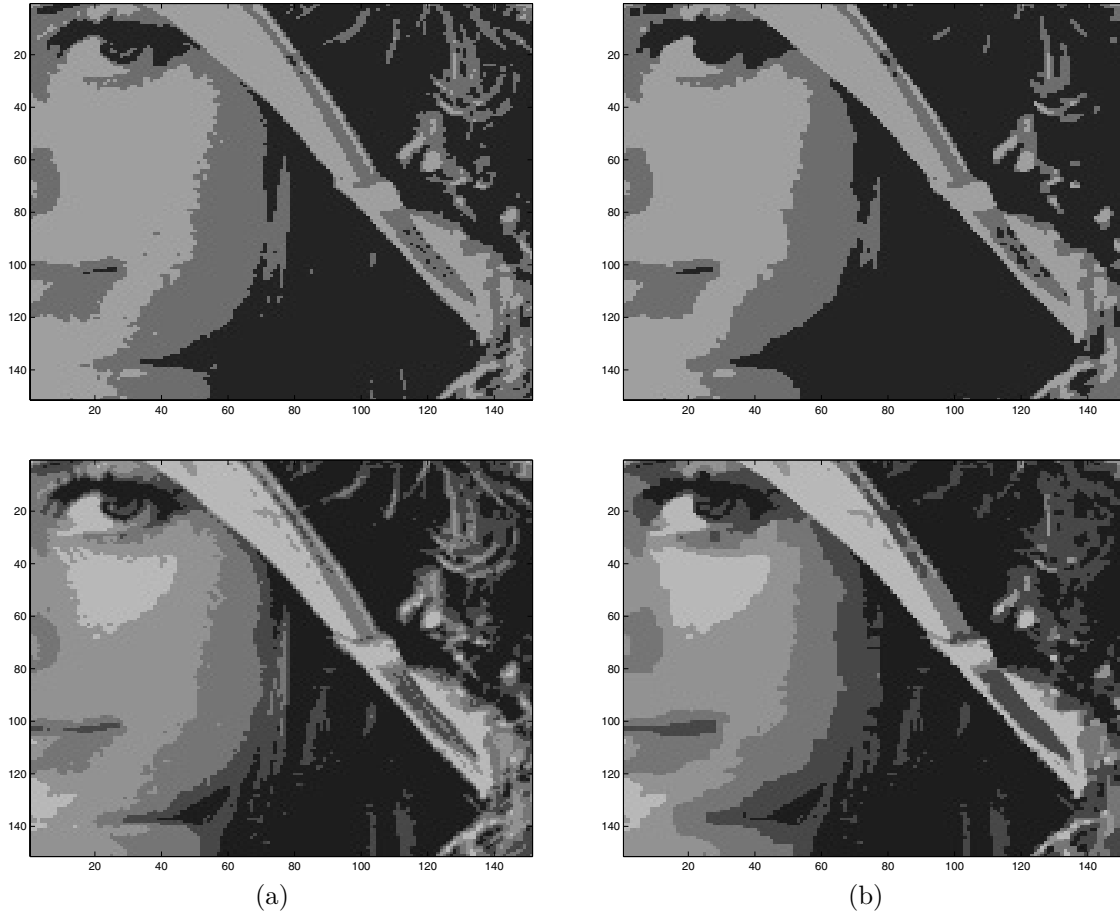


FIGURE 3.  $n$ -classes classified images obtained using the topological gradient algorithm:  $n = 3$  and  $C = \{34; 112; 165\}$  (top) and  $n = 5$  and  $C = \{29; 71; 117; 146; 184\}$  (bottom); unregularized (a) and regularized (b).

of the topological asymptotic analysis to the image restoration problem, and then we use these results in order to obtain a classified image with smoother contours. This section could be considered as an introducing step of the final algorithm presented in Section 5.

#### 4.1. Image restoration and smoothing using the topological gradient theory

Let  $\Omega$  be an open bounded domain of  $\mathbb{R}^2$  and  $j(\Omega) = J(u_\Omega)$  be a cost function to be minimized, where  $u_\Omega$  is the solution to a given PDE problem defined in  $\Omega$ . For a small  $\rho \geq 0$ , let  $\Omega_\rho = \Omega \setminus \overline{\sigma}_\rho$  the perturbed domain by the insertion of a crack  $\sigma_\rho = x_0 + \rho\sigma(n)$ , where  $x_0 \in \Omega$ ,  $\sigma(n)$  is a straight crack, and  $n$  a unit vector normal to the crack. We assume that the crack is 2-dimensional, and its shape is for example a flat ellipsoid.

Consider now the following partial differential equation

$$\begin{cases} -\operatorname{div}(c\nabla u) + u = u_0 & \text{in } \Omega, \\ \partial_n u = 0 & \text{on } \partial\Omega. \end{cases} \tag{14}$$

This PDE has a unique solution  $u \in H^1(\Omega)$  if  $u_0 \in L^2(\Omega)$  and if  $c \in L^\infty(\Omega)$  and  $c > \delta > 0$  [13].

The solution  $u_\rho \in H^1(\Omega_\rho)$  of the perturbed problem satisfies

$$\begin{cases} -\operatorname{div}(c\nabla u_\rho) + u_\rho = u_0 & \text{in } \Omega_\rho, \\ \partial_n u_\rho = 0 & \text{on } \partial\Omega_\rho. \end{cases} \quad (15)$$

The variational formulation of (15) is

$$\begin{cases} \text{Find } u_\rho \in H^1(\Omega_\rho) \text{ so that} \\ a_\rho(u_\rho, w) = l_\rho(w), \quad \forall w \in H^1(\Omega_\rho), \end{cases} \quad (16)$$

where  $a_\rho$  is the following bilinear form, defined on  $H^1(\Omega_\rho)^2$

$$a_\rho(u, w) = \int_{\Omega_\rho} (c\nabla u \nabla w + uw) \, dx, \quad (17)$$

and  $l_\rho$  is the linear form defined on  $L^2(\Omega_\rho)$

$$l_\rho(w) = \int_{\Omega_\rho} u_0 w \, dx. \quad (18)$$

We consider the following cost function

$$J(u_\rho) = \int_{\Omega_\rho} \|\nabla u_\rho\|^2 \, dx, \quad (19)$$

where  $u_\rho$  is the solution of the equation (16). The idea is to find the edge set of the image, to preserve it, and to smooth the image outwards thanks to the Laplace equation in (15). This is justified by the fact that most of the main edges of the original image will be part of the interfaces of the classified image. Hence, in order to find the contours of the image, the cost function is chosen to minimize the energy out of the contours ( $\sigma_\rho$  will represent the edge set). We can rewrite  $J$  as a function of  $\rho$  by considering the following map:

$$j : \rho \mapsto \Omega_\rho \mapsto u_\rho \mapsto j(\rho) := J(u_\rho). \quad (20)$$

In order to apply the topological asymptotic theory, we have to verify the following hypothesis [6, 27].

**Theorem 4.1.** *If there exists a linear form  $L_\rho$  defined on  $L^2(\Omega)$ , a function  $f : \mathbb{R}^+ \rightarrow \mathbb{R}^+$ , and four real numbers  $\delta J_1$ ,  $\delta J_2$ ,  $\delta a$  and  $\delta l$  so that*

- (1)  $\lim_{\rho \rightarrow 0} f(\rho) = 0$ ;
- (2)  $J_\rho(u_\rho) - J_\rho(u_0) = L_\rho(u_\rho - u_0) + f(\rho)\delta J_1 + o(f(\rho))$ ;
- (3)  $J_\rho(u_0) - J_0(u_0) = f(\rho)\delta J_2 + o(f(\rho))$ ;
- (4)  $(a_\rho - a_0)(u_0, v_\rho) = f(\rho)\delta a + o(f(\rho))$ ;
- (5)  $(l_\rho - l_0)(v_\rho) = f(\rho)\delta l + o(f(\rho))$ ,

where the adjoint state  $v_\rho$  is solution of the adjoint equation

$$a_\rho(w, v_\rho) = -L_\rho(w) \quad \forall w \in L^2(\Omega), \quad (21)$$

and  $u_\rho$  is solution of the direct equation

$$a_\rho(u_\rho, w) = l_\rho(w) \quad \forall w \in L^2(\Omega). \quad (22)$$

Then the cost function has the following asymptotic expansion

$$j(\rho) - j(0) = f(\rho)g(x) + o(f(\rho)), \quad (23)$$



where  $g(x)$  is the topological gradient, given by

$$g(x) = \delta J_1 + \delta J_2 + \delta a - \delta l. \tag{24}$$

In the present case, if we denote by  $v$  the adjoint state, solution of the adjoint problem

$$\begin{cases} -\operatorname{div}(c\nabla v) + v = -\partial_u J(u) & \text{in } \Omega, \\ \partial_n v = 0 & \text{on } \partial\Omega, \end{cases} \tag{25}$$

we can apply Theorem 4.1, and we obtain the following topological asymptotic expansion [6, 20]

$$j(\rho) - j(0) = \rho^2 G(x_0, n) + o(\rho^2), \tag{26}$$

with

$$G(x_0, n) = -\pi(\nabla u(x_0) \cdot n)(\nabla v(x_0) \cdot n) - \pi|\nabla u(x_0) \cdot n|^2. \tag{27}$$

Then the topological gradient could be written as

$$G(x, n) = \langle M(x)n, n \rangle, \tag{28}$$

where  $M(x)$  is the symmetric matrix defined by

$$M(x) = -\pi \frac{\nabla u(x)\nabla v(x)^T + \nabla v(x)\nabla u(x)^T}{2} - \pi \nabla u(x)\nabla u(x)^T. \tag{29}$$

The goal is to minimize the cost function, and hence the idea is to find the points  $x_0$  (and the corresponding unit vector  $n$ ) for which the topological gradient is negative. In this case, equation (26) ensures the asymptotic decrease of the cost function if we insert a small crack at these points.

For a given  $x$ ,  $G(x, n)$  takes its minimal value when  $n$  is the eigenvector associated to the lowest eigenvalue  $\lambda_{min}$  of  $M$ . This value will be considered as the topological gradient associated to the optimal orientation of the crack  $\sigma_\rho(n)$ .

From the numerical point of view, it is not so easy to implement cracks. We aren't going to create a new finite element model with mesh refinement around the cracks. When  $\lambda_{min}$  is smaller than a given threshold, it tells us that the pixel is located on the edges of the image. For image restoration, we just set the value of  $c$  to 0 (or to  $\varepsilon$ ) in that pixel.

The restoration algorithm is the following:

**Algorithm**

- Initialization:  $c = c_0 > 0$  everywhere.
- Calculation of  $u$  and  $v$ : solutions of the direct (14) and adjoint (25) problems corresponding to this value of  $c$ .
- Computation of the  $2 \times 2$  matrix  $M$  and its lowest eigenvalue  $\lambda_{min}$  at each point of the domain.
- Set

$$c = \begin{cases} 0 & \text{if } x \in \Omega \text{ such that } \lambda_{min} < -\eta < 0, \\ c_0 & \text{elsewhere.} \end{cases} \tag{30}$$

- Calculation of  $u_1$  solution to problem (14) with this new value of  $c$ .
- Application of the closest class algorithm to  $u_1$ .

One can see [20] for more details.

This algorithm finds the contours of the image, and smoothes the image everywhere else. The idea is then to simply apply the closest class algorithm to the smothered image  $u_1$ . The constant  $c_0$  plays the same role as  $\alpha$  in the previous section. It controls the regularity of the restored image and then the length of the interfaces.

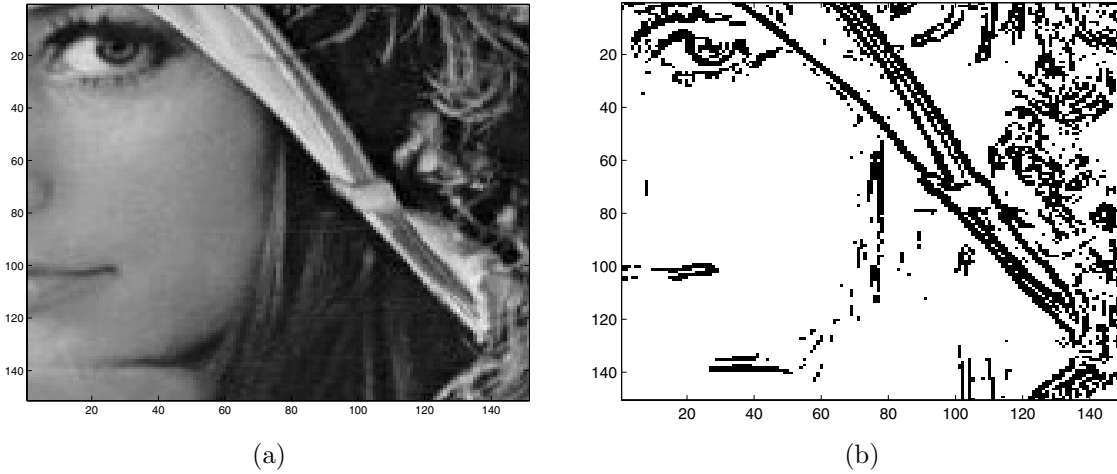


FIGURE 4. Original image (a); identified edges by the topological gradient algorithm (b).

No convergence to a global minimum could be ensured.

**Remark.** As the first resolution of the direct problem is performed with a constant value of  $c$ , it is possible to largely accelerate the computation by using the DCT (Discrete Cosine Transform) method. If we consider the following cosine basis

$$\phi_{m,n} = \delta_{m,n} \cos(m\pi x) \cos(n\pi y)$$

where  $\delta_{m,n}$  are appropriate normalisation coefficients, equation (14) is equivalent to

$$\sum_{m,n} (1 + c(m\pi)^2 + c(n\pi)^2) u_{m,n} \phi_{m,n} = \sum_{m,n} u_{0m,n} \phi_{m,n}, \quad (31)$$

where  $(u_{0m,n})$  represents DCT coefficients of the original image  $u_0$ . It is then straightforward to identify  $(u_{nm})$ , the DCT coefficients of  $u$  in (31), and then to compute  $u$  using an inverse DCT. The complexity of this resolution is  $\mathcal{O}(N \log(N))$  where  $N$  is the size of the image (*i.e.* the number of pixels). Then, for the second resolution of the direct problem with a non constant  $c$ , the DCT solver is used as a preconditioner to the conjugate gradient algorithm. This works very well because  $c$  is close to a constant; it is equal to  $c_0$  except on the edges of the image, see [20] for more details.

## 4.2. Numerical results

From a numerical point of view, we took  $c_0 = 1$ , and in order to avoid numerical illposedness, we set

$$c = \varepsilon \text{ if } x \in \Omega \text{ such that } \lambda_{\min} < -\eta < 0 \quad (32)$$

instead of  $c = 0$  in the previous algorithm, where  $\varepsilon$  is a small positive constant.

Figure 4 shows the original image (a), and its identified edges by the previous algorithm (b). When the most negative eigenvalue is smaller than the threshold  $-\eta$ , the pixel appears in black on this figure. One can see that the main contours of the image are well identified.

Figure 5a shows the restored image using the second part of the topological gradient algorithm for image restoration. Figure 5b shows the result of the closest class algorithm applied to Figure 5a with  $n = 2$  classes ( $C = \{0; 255\}$ ). Figure 5b should be compared to Figure 2b. The smoothing of contours and the number of

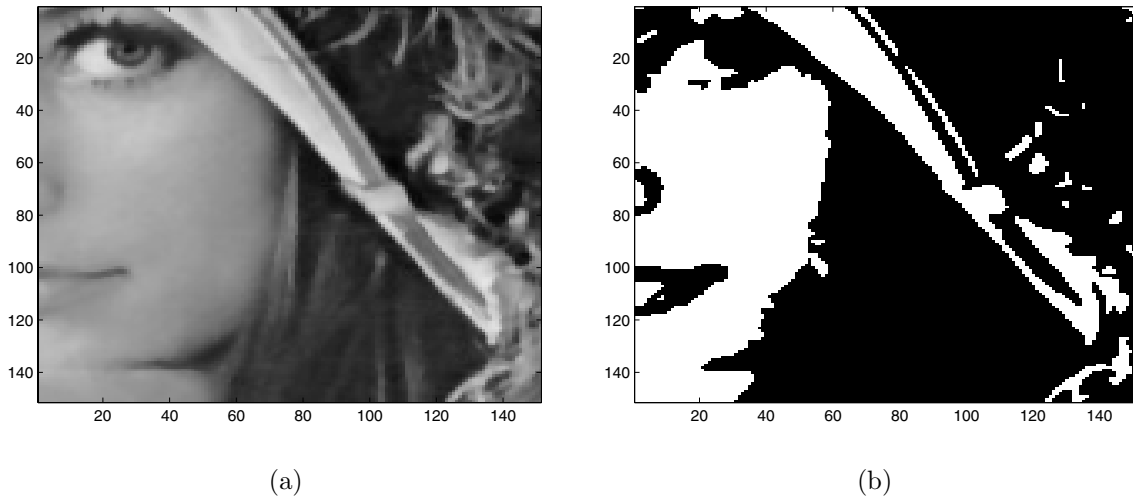


FIGURE 5. Two-classes classified image obtained using the topological gradient algorithm for smoothing (a) and then the closest class algorithm for classification (b).

isolated points are more or less the same, but our latest algorithm needs only one iteration of the topological gradient, whereas the algorithm described in the previous section needed to be iterated. Although it is possible to iterate the topological gradient algorithm for image restoration, it does not improve appreciably the smoothing of the classified image, whereas it is unavoidable to iterate a few times this process in the previous section's algorithm.

Figure 6 shows the same results as in Figure 5 for 3 and 5 classes (the smooth image obtained using the topological gradient is the same as in the 2-classes case).

## 5. AN IMPROVEMENT TO THE PREVIOUS ALGORITHM

In this section, we propose a significant improvement to the previous algorithm. It still consists firstly in an iteration of the topological asymptotic analysis (but for a different partial differential equation) for the image smoothing and secondly in the closest class algorithm for its classification.

### 5.1. Another way to use the topological asymptotic expansion for image smoothing

We still consider the following partial differential equation

$$\begin{cases} -\operatorname{div}(c\nabla u) + u = u_0 & \text{in } \Omega, \\ \partial_n u = 0 & \text{on } \partial\Omega. \end{cases} \quad (33)$$

Instead of setting  $c = 0$  (or  $c = \varepsilon$  from a numerical point of view) on the edge set and  $c = c_0$  elsewhere, we set

$$c = \begin{cases} c = 0 \text{ (or } \varepsilon) & \text{on the edge set,} \\ c \sim +\infty \text{ (e.g. } c = \frac{c_0}{\varepsilon}) & \text{elsewhere.} \end{cases} \quad (34)$$

In comparison with the previous section, the topological gradient  $g(x)$  and the general algorithm remains unchanged. In particular, the edge set is given by thresholding  $\lambda_{min}$ .

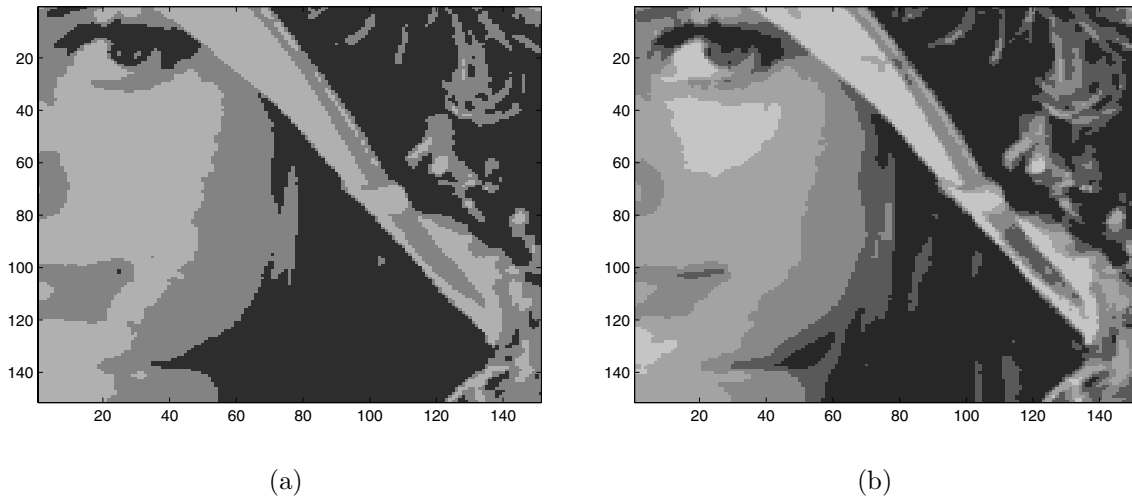


FIGURE 6.  $n$ -classes classified images obtained using the topological gradient algorithm for smoothing and then the closest class algorithm for classification:  $n = 3$  and  $C = \{34; 112; 165\}$  (a) and  $n = 5$  and  $C = \{29; 71; 117; 146; 184\}$  (b).

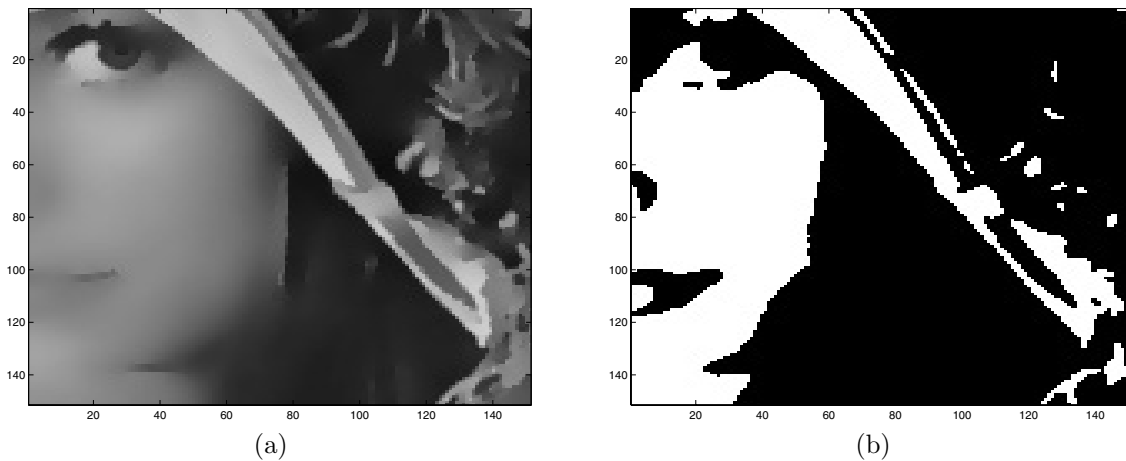


FIGURE 7. Two-classes classified image obtained using the topological gradient algorithm applied to the new equation for smoothing (a) and then the closest class algorithm for classification (b).

From a numerical point of view, as  $\varepsilon$  is supposed to be small, if we are on a contour,  $c = \varepsilon$  and then  $u$  and  $u_0$  are close. But otherwise,  $c = \frac{c_0}{\varepsilon}$  and then the P.D.E. is nearly equivalent to  $\Delta u = 0$ , which will provide a really smooth image.

## 5.2. Numerical results

Figure 7a shows the computed image using the topological gradient algorithm applied to our new equation. Figure 7b shows the result of the closest class algorithm applied to Figure 7a with  $n = 2$  classes ( $C = \{0; 255\}$ ). Figure 7b should be compared to Figure 2b and Figure 5b. We can see that the smoothing of contours is much

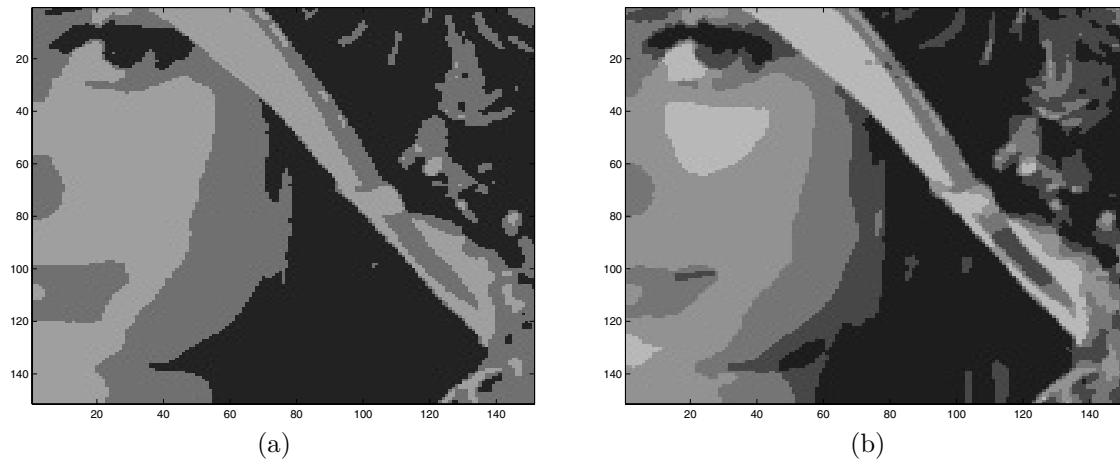


FIGURE 8.  $n$ -classes classified images obtained using the topological gradient algorithm applied to the new equation for smoothing and then the closest class algorithm for classification:  $n = 3$  and  $C = \{34; 112; 165\}$  (a) and  $n = 5$  and  $C = \{29; 71; 117; 146; 184\}$  (b).

more efficient in this case, and the computational cost of our latest algorithm is exactly the same as the previous one (only one iteration of topological gradient computation).

Figure 8 shows the same results as in Figure 7 for 3 and 5 classes. We still observe much smoother contours.

### 5.3. Impact of noise

In this subsection, we study the impact of noise on the classified image. We performed three experiments, with three different levels of additive white Gaussian noise. For each experiment, the SNR (signal to noise ratio) is given, and it is equal to 20, 15 and 10 respectively. Figure 9 shows for each level of noise the original (noisy) image, and the classified image. We still use  $n = 5$  classes and  $C = \{29; 71; 117; 146; 184\}$ .

We can notice that our algorithm is quite robust when the level of noise increases. Although the interfaces are no more very smooth in the case of a high noise level ( $SNR = 10$ ), the quality of the classified image remains good. In the case of a reasonable level of noise ( $SNR = 20$ ), there are not much differences with the case without noise.

## 6. CONCLUDING REMARKS

### 6.1. Comparison between the different methods

We have presented in this paper different ways to both classify and regularize grey-level images. Table 1 gives the computational cost, the square difference between the original and classified images, and the smoothness of the contours (value of the regularization term in the cost function) for the different algorithms and for the different number of classes. Our last method is obviously the most efficient of all regularization methods. Another interesting point is that the two restoration-based methods have a computational cost that is independent from the number of classes. Once the image regularized, the classification is done by the closest class algorithm, which computational cost is negligible compared to the regularization computational cost. The regularization cost is almost the same for the two last methods, but the lengths of interfaces clearly confirm that the last method gives a much smoother image.

Figure 10 allows one to compare the  $n$ -classes (with  $n = 5$  and  $C = \{29; 71; 117; 146; 184\}$ ) classified images computed with these different algorithms. This figure clearly confirm the results shown in Table 1 about the length of the interfaces.



FIGURE 9. Noisy images (a) and 5-classes ( $C = \{29; 71; 117; 146; 184\}$ ) classified images obtained using the topological method applied to the improved restoration method (b), for different levels of noise (top:  $SNR = 20$ ; middle:  $SNR = 15$ ; bottom:  $SNR = 10$ ).

TABLE 1. Computational cost (time in seconds), discrepancy between the original and classified images, and length of the interfaces for the different algorithms and number of classes.

Number of classes	$n = 2$ $C = \{0; 255\}$	$n = 3$ $C = \{34; 112; 165\}$	$n = 5$ $C = \{29; 71; 117; 146; 184\}$
Closest class algorithm (no regularization)	$t = 0.02$ $ u - u_0 ^2 = 5836$ $ \Gamma  = 2358$	$t = 0.06$ $ u - u_0 ^2 = 903$ $ \Gamma  = 4513$	$t = 0.05$ $ u - u_0 ^2 = 591$ $ \Gamma  = 7913$
Topological gradient for the cost function with regularization	$t = 12.67$ $ u - u_0 ^2 = 7421$ $ \Gamma  = 2069$	$t = 45.63$ $ u - u_0 ^2 = 1102$ $ \Gamma  = 3872$	$t = 81.78$ $ u - u_0 ^2 = 890$ $ \Gamma  = 5770$
Restoration method (by topological gradient) + closest class	$t = 34.69$ $ u - u_0 ^2 = 10\,580$ $ \Gamma  = 1810$	$t = 34.73$ $ u - u_0 ^2 = 2657$ $ \Gamma  = 3414$	$t = 34.72$ $ u - u_0 ^2 = 1702$ $ \Gamma  = 5954$
Improved restor. method (by topological gradient) + closest class	$t = 37.16$ $ u - u_0 ^2 = 10\,791$ $ \Gamma  = 1566$	$t = 37.17$ $ u - u_0 ^2 = 2504$ $ \Gamma  = 2870$	$t = 37.17$ $ u - u_0 ^2 = 1684$ $ \Gamma  = 4839$

Finally, Figure 11 shows the square difference between the classified images and the original image *versus* the length of the interfaces for the four algorithms presented in this paper. For each method, the three points correspond to the three numerical experiments  $n = 2$ ,  $n = 3$  and  $n = 5$  classes summarized in Table 1. If one is interested in a very smooth classified image, the last method is clearly the most appropriate one, but if the main goal is not the regularization of the classified image, one should use the second algorithm. We can also remark that adding a regularization term in the closest class algorithm does not degrade too much the square difference with the original image, and that the improved restoration method gives much better results than the original restoration method because the interfaces' length and the square difference with the original image both decrease.

### 6.2. Unsupervised classification

If the number  $n$  of classes is given, but not their values  $C := (C_i)_{i=1,\dots,n}$ , it is possible to determine them in an optimal way. This classification problem could be defined as

$$\min_{\omega, C} j(\omega, C) = \int_{\Omega} |u - u_0|^2 \, dx + \alpha \sum_{i \neq j} |\Gamma_{ij}|. \tag{35}$$

In order to point out the role of  $C$  in this problem, we can write it in a different way

$$\min_{\omega, C} j(\omega, C) = \sum_{i=1}^n \left( \int_{\omega_i} |C_i - u_0|^2 \, dx \right) + \alpha \sum_{i \neq j} |\Gamma_{ij}|. \tag{36}$$

The basic idea is to start with an initial guess of  $C$ , then to minimize  $j(\omega, C)$  alternatively with respect to  $\omega$  and with respect to  $C$ . The minimization with respect to  $C$  is obtained straightforward by the mean of  $u_0$  in

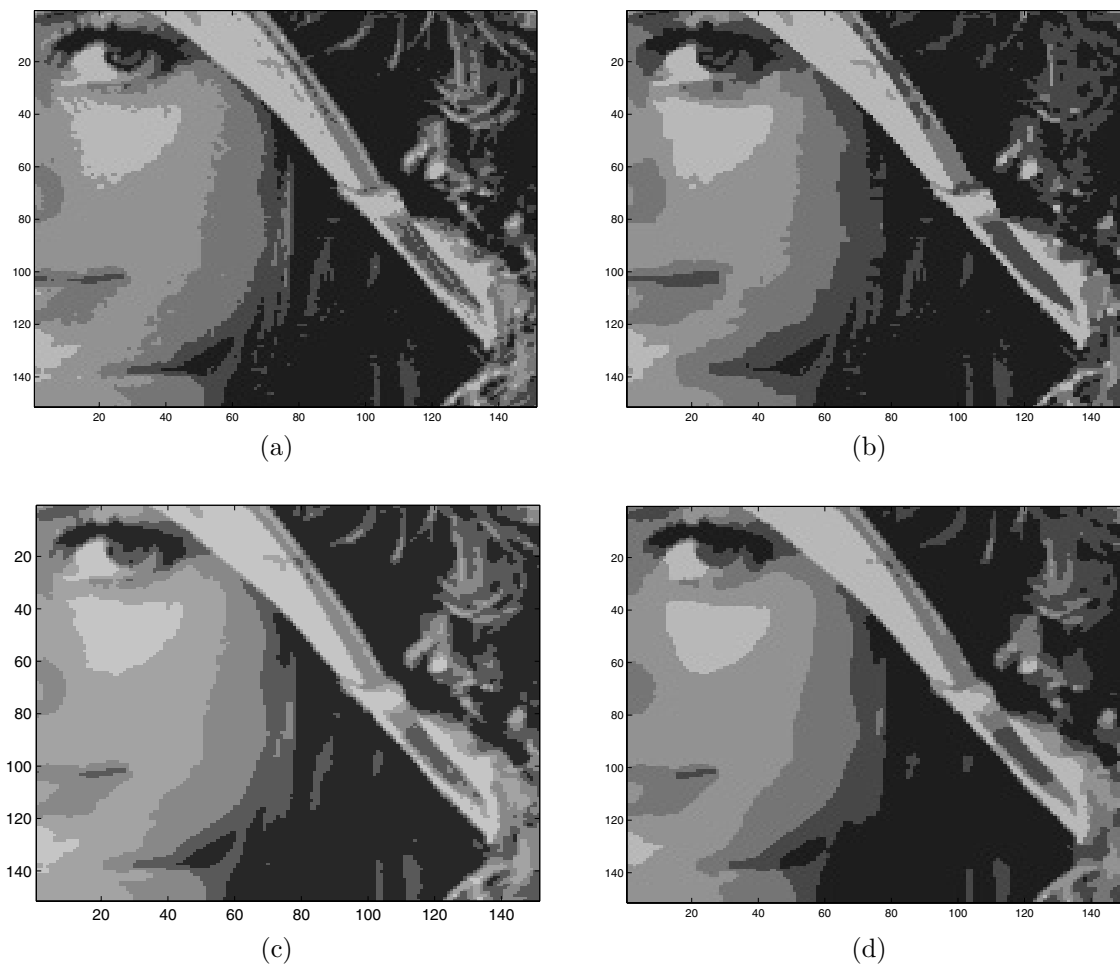


FIGURE 10. 5-classes ( $C = \{29; 71; 117; 146; 184\}$ ) classified images obtained using: the closest class algorithm (no regularization) (a), the topological gradient method for the computation of the exact variation of the cost function (with regularization) (b), the closest class algorithm applied to the restored image (by the topological gradient method) (c), and the closest class algorithm applied to the restored image (by the improved topological gradient method) (d).

each class:

$$C_i = \frac{1}{|\omega_i|} \int_{\omega_i} u_0 \, dx. \quad (37)$$

More precisely, this algorithm is as follows:

#### Algorithm

- Define an initial guess  $C$ .
  - Repeat until convergence:
    - Calculate the classified image  $u_0$  using  $C$ .
    - Update the values of  $C$  using (37).
- End repeat.



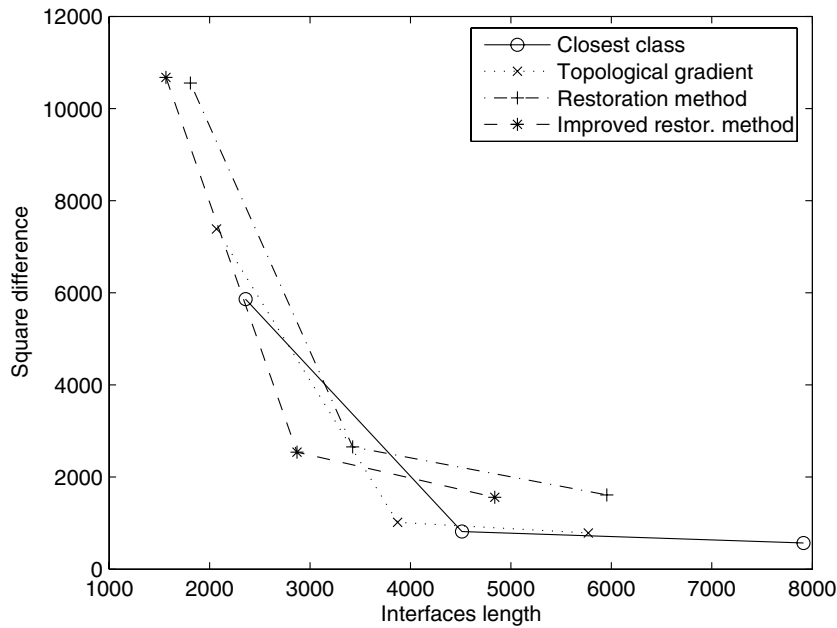


FIGURE 11. Square difference between the classified images and the original image *versus* the length of the interfaces for the different algorithms.

We used this algorithm to find the values we used in the case of 3 and 5-classes classification:  $C = \{34; 112; 165\}$  and  $C = \{29; 71; 117; 146; 184\}$  respectively. The algorithm provided these values for a negligible computation cost (much less than one second) in the unregularized case ( $\alpha = 0$ ).

If the number  $n$  of classes is not given, we can add a penalization term in the cost function, measuring the number of classes:

$$j(\omega) = \sum_{i=1}^n \left( \int_{\omega_i} |C_i - u_0|^2 dx \right) + \alpha \sum_{i \neq j} |\Gamma_{ij}| + \beta n, \tag{38}$$

where  $\beta$  is a positive weighting coefficient. As in the previous paragraph, it is possible to compute explicitly the impact of adding an extra class (or removing a class) on this cost function, and the previous algorithm provides then the number and values of the classes.

One should notice that if  $\beta$  is chosen quite small, then the algorithm will provide a high number of classes, and then a quite precise classified image, whereas if  $\beta$  is chosen larger, the number of classes will be small, and the classified image will not be very close to the original image.

### 6.3. Future prospects

One of our main goals is now to extend these methods to color images and also to three-dimensional images. In the case of color images, some preliminary works showed that a decomposition of the image into the HSV (hue-saturation-value) space gives promising results. We first divide up the image into three separate channels. Each of these channels can be seen as a grey level image, and hence classified using for example our improved algorithm. Finally the three classified channels are recombined to form a color classified image.

## REFERENCES

- [1] G. Allaire, *Shape optimization by the homogenization method*. Applied Mathematical Sciences **146**, Springer (2002).
- [2] G. Allaire and R. Kohn, Optimal design for minimum weight and compliance in plane stress using extremal microstructures. *Eur. J. Mech. A Solids* **12** (1993) 839–878.
- [3] G. Allaire, F. Jouve and A.-M. Toader, A level-set method for shape optimization. *C. R. Acad. Sci. Sér. I* **334** (2002) 1125–1130.
- [4] G. Allaire, F. de Gournay, F. Jouve and A.-M. Toader, *Structural optimization using topological and shape sensitivity via a level set method*, Internal report, n° 555, CMAP, École polytechnique. *Control Cybern.* **34** (2005) 59–80.
- [5] H. Ammari, M.S. Vogelius and D. Volkov, Asymptotic formulas for perturbations in the electromagnetic fields due to the presence of inhomogeneities of small diameter II - The full Maxwell equations. *J. Math. Pures Appl.* **80** (2001) 769–814.
- [6] S. Amstutz, I. Horchani and M. Masmoudi, Crack detection by the topological gradient method. *Control Cybern.* **34** (2005) 119–138.
- [7] G. Aubert and J.-F. Aujol, Optimal partitions, regularized solutions, and application to image classification. *Appl. Anal.* **84** (2005) 15–35.
- [8] G. Aubert and P. Kornprobst, *Mathematical problems in image processing*. Applied Mathematical Sciences **147**, Springer-Verlag, New York (2002).
- [9] J.-F. Aujol, G. Aubert and L. Blanc-Féraud, Wavelet-based level set evolution for classification of textured images. *IEEE Trans. Image Process.* **12** (2003) 1634–1641.
- [10] M. Bendsoe, *Optimal topology design of continuum structure: an introduction*. Technical report, Department of Mathematics, Technical University of Denmark, Lyngby, Denmark (1996).
- [11] M. Berthod, Z. Kato, S. Yu and J. Zerubia, Bayesian image classification using Markov random fields. *Image Vision Comput.* **14** (1996) 285–293.
- [12] C.A. Bouman and M. Shapiro, A multiscale random field model for Bayesian image segmentation. *IEEE Trans. Image Process.* **3** (1994) 162–177.
- [13] P.G. Ciarlet, *Finite Element Method for Elliptic Problems*. North Holland (2002).
- [14] L. Cohen, E. Bardinet and N. Ayache, Surface reconstruction using active contour models. *SPIE Int. Symp. Optics, Imaging and Instrumentation*, San Diego California USA (July 1993).
- [15] R. Dautray and J.-L. Lions, *Analyse mathématique et calcul numérique pour les sciences et les techniques*. Collection CEA, Masson, Paris (1987).
- [16] X. Descombes, R. Morris and J. Zerubia, Some improvements to Bayesian image segmentation – Part one: modelling. *Traitement du signal* **14** (1997) 373–382.
- [17] X. Descombes, R. Morris and J. Zerubia, Some improvements to Bayesian image segmentation – Part two: classification. *Traitement du signal* **14** (1997) 383–395.
- [18] A. Friedman and M.S. Vogelius, Identification of small inhomogeneities of extreme conductivity by boundary measurements: a theorem of continuous dependence. *Arch. Rational Mech. Anal.* **105** (1989) 299–326.
- [19] S. Garreau, P. Guillaume and M. Masmoudi, The topological asymptotic for PDE systems: The elasticity case. *SIAM J. Control Optim.* **39** (1991) 17–49.
- [20] L. Jaafar Belaid, M. Jaoua, M. Masmoudi and L. Siala, Image restoration and edge detection by topological asymptotic expansion. *C. R. Acad. Sci. Paris. Ser. I Math.* **342** (2006) 313–318.
- [21] Z. Kato, *Modélisations markoviennes multirésolutions en vision par ordinateur - Application à la segmentation d'images SPOT*. Ph.D. thesis, INRIA, Sophia Antipolis, France (1994).
- [22] M. Masmoudi, The topological asymptotic, in *Computational Methods for Control Applications*, R. Glowinski, H. Karawada and J. Periaux Eds., *GAKUTO Internat. Ser. Math. Sci. Appl.* **16**, Tokyo, Japan (2001) 53–72.
- [23] D. Mumford and J. Shah, Optimal approximations by piecewise smooth functions and associated variational problems. *Comm. Pure Appl. Math.* **42** (1989) 577–685.
- [24] N. Paragios and R. Deriche, Geodesic active regions and level set methods for supervised texture segmentation. *Int. Jour. Computer Vision* **46** (2002) 223–247.
- [25] T. Pavlidis and Y.-T. Liow, Integrating region growing and edge detection. *IEEE Trans. Pattern Anal. Machine Intelligence* **12** (1990) 225–233.
- [26] P. Perona and J. Malik, Scale-space and edge detection using anisotropic diffusion. *IEEE Trans. Pattern Anal. Machine Intelligence* **12** (1990) 629–638.
- [27] B. Samet, S. Amstutz and M. Masmoudi, The topological asymptotic for the Helmholtz equation. *SIAM J. Control Optim.* **42** (2003) 1523–1544.
- [28] C. Samson, L. Blanc-Féraud, G. Aubert and J. Zerubia, A level set method for image classification. *Int. J. Comput. Vision* **40** (2000) 187–197.
- [29] C. Samson, L. Blanc-Féraud, G. Aubert and J. Zerubia, A variational model for image classification and restauration. *IEEE Trans. Pattern Anal. Machine Intelligence* **22** (2000) 460–472.

- [30] J.A. Sethian, *Level set methods evolving interfaces in geometry, fluid mechanics, computer vision, and materials science*. Cambridge University Press (1996).
- [31] J. Sokolowski and A. Zochowski, Topological derivatives of shape functionals for elasticity systems. *Int. Ser. Numer. Math.* **139** (2002) 231–244.
- [32] S. Solimini and J.M. Morel, *Variational methods in image segmentation*. Birkhauser (1995).
- [33] L. Vese and T. Chan, *Reduced Non-Convex Functional Approximations for Image Restoration and Segmentation*. UCLA CAM Report 97–56 (1997).
- [34] M.Y. Wang, D. Wang and A. Guo, A level set method for structural topology optimization. *Comput. Methods Appl. Mech. Engrg.* **192** (2003) 227–246.
- [35] J. Weickert, Efficient image segmentation using partial differential equations and morphology. *Pattern Recogn.* **34** (2001) 1813–1824.